



Development of porous silicon matrix and characteristics of porous silicon/tin oxide structures

V.S. Vidhya^a, P. Padmavathy^b, K.R. Murali^c, C. Sanjeeviraja^b, P. Manisankar^a, M. Jayachandran^{c,*}

^a School of Chemistry, Alagappa University, Karaikudi-630 003, India

^b School of Physics, Alagappa University, Karaikudi-630 003, India

^c Electrochemical Materials Science Division, Central Electrochemical Research Institute, Karaikudi-630 006 (Council of Scientific and Industrial Research, New Delhi), India

ARTICLE INFO

Article history:

Received 7 March 2010

Received in revised form 30 December 2010

Available online 25 January 2011

Keywords:

PSi;

Electrochemical etching;

Tin oxide

ABSTRACT

Porous silicon (PSi) was formed at different current densities in the range of 5–60 mA/cm² by electrochemical anodized etching in HF for different durations in the range of 10–30 min. Above this PSi structure, SnO₂ films were deposited by the spin coating technique. The PSi has been characterized by X-ray diffraction studies. Peaks pertaining to PSi along with those corresponding to SnO₂ are observed. Atomic force microscopic studies indicate that very fine needle like silicon nanostructures are observed which is the result of the best PSi structure formed at 30 mA/cm². For the SnO₂ covered PSi structures, larger grains are observed with uniform coverage. The PSi samples prepared at current densities above and below 30 mA/cm² show PL spectra with asymmetric and overlapped peaks. The PL profile of thin SnO₂ film coated on PSi shows a peak at 633 nm and a small hump at about 660 nm.

© 2011 Elsevier B.V. All rights reserved.

1. Introduction

Porous silicon (PSi) can be formed by an anodic electrochemical etching technology on single crystal Si surface in hydrofluoric acid (HF) mixed solutions [1,2]. This process forms a sponge like porous layer of interconnected 1–10 nm nanocrystalline texture features on the surface. PSi may show size dependent discrete excited states due to quantum confinement effect, as well as pronounced changes in other physical, chemical and material properties due to large surface to volume ratio [1]. When PSi contains quantized size particles, it acquires a broadening of its effective energy gap leading to a room temperature luminescence in the visible wavelength range [3]. In addition, its porous structure possesses intermediate refractive index between those of crystalline Si and air [4]. Therefore, a thin PSi film can act as an efficient antireflection coating (ARC) with enhanced light transmission properties.

The potentiality of integrating the PSi in a crystalline Si solar cell is enormous [5]. High solar energy conversion efficiency cells around 13–14% with the outer part of the emitter made porous, have recently been obtained. Hence the possibilities to optimize modify and improve the performances are numerous [6]. This is owing to the fact that as soon as PSi is formed and dried, the hydrogen passivated surface is slowly replaced by native oxides. Therefore, development of a controlled oxidation process is seminal to stabilize the properties of PSi.

Moreover, single and multicrystalline silicon does not show sensitivity at all to inflammable or hazardous gases. But, when the silicon substrate can be prepared with porous structure, it offers several advantages: porous silicon has a large specific surface area (200–1000 m²/cm³), which provides high sensitivity to external gaseous molecules (for example, to hydrogen [7,8]); it can be used to produce a low cost, compact sensor system on a silicon chip, where both the sensing part (the porous silicon) and the transducer part can be integrated. At the same time it is well known that the parameters of porous silicon degrade with time, which means that porous silicon gas sensors cannot fulfil the durability requirement. In this paper we propose a method for protecting the porous silicon layer from ambient air, in order to prevent it from further degradation with time. In this regard, we have studied the effect of incorporating SnO₂:F films into PSi structure. PSi layers on p-type Si with optimum porous structure have been developed, their structural, chemical and PL properties are studied and the influence of SnO₂ films on these properties are reported.

2. Experimental procedure

Porous silicon samples were formed from p-type Si (100), 0.05–0.07 Ωcm wafer by electrochemical etching. A 1:2 mixture of 30% hydrofluoric acid and ethanol was used as electrolyte. Aluminium foil was mounted on the back side of the samples to improve the uniformity of the anodic current. Galvanostatic etching was carried out for 30 min with the current densities of 5, 10, 30, 45 and 60 mA/cm² in the dark by using an Autolab electrochemical work station. The weight of the silicon wafer before etching was measured by using a Mettler semi micro

* Corresponding author. Tel.: +91 4565 227550 559.

E-mail address: mjayam54@yahoo.com (M. Jayachandran).

balance and the weight of the silicon after etching was measured. The difference in weight is a measure of the porosity. The required precursor solution was prepared by dissolving stannic chloride ($\text{SnCl}_4 \cdot 5\text{H}_2\text{O}$) in 50 ml of ethanol adding a few drops of hydrochloric acid as a catalyst. This solution is refluxed at 60°C for 2 h and left in an open beaker to gelate. After allowing two days for gelation, the sol–gel obtained is used for preparing the precursor coatings on glass substrates and further heating of the coatings yields tin oxide films.

The glass substrate on which porous silicon wafers were fixed, was placed on the turntable symmetrically with respect to the central hole in the turntable, which is connected to a rotary vacuum pump. Under vacuum, the substrate gets firmly attached to the turntable and does not come out even when the turntable spin rate reaches 3000 rpm. The selected turntable spin rate and time are fed into the spin coating unit through the PC. After 5 to 6 drops of sol–gel are placed at the centre of the substrate, the unit is switched on. The turntable starts spinning at the pre-determined rate and automatically stops at the end of the programmed time fed into the unit. During the high spin speed centrifugal forces drive the liquid radially outwards and the pores are filled with the gel. Excess material is driven off from the edges of the PSi wafer but the remainder is retained inside the pores and surface as a very thin layer by the viscous and surface tension forces.

The Gel/PSi coated substrates were placed inside the furnace, where the desired heat treatment temperature of 400°C was already maintained and heated for 15 min. This heating step results in the formation of tin oxide films and these SnO_2 /PSi structures were further characterized for their PL and structural studies.

3. Results and discussion

As far as PSi is concerned it is expected that the anodic etching route of porous structure formation on silicon single crystalline substrate does not lead to deterioration of crystal structure [9,10,16,17].

PSi structures are formed on p-type silicon single crystal wafers with (400) orientation. Fig. 1b, c, d, e and f shows the XRD pattern for the surfaces etched at current densities of 5, 10, 30, 45 and 60 mA/cm^2 respectively along with the sharp and highly intense (400) peak at $2\theta = 69.9^\circ$ and also seen in Fig. 1a corresponding to silicon single crystal. XRD patterns show distinctive behaviour between the single crystal surface and the etched surface. At the very low current density of 5 mA/cm^2 , the etching force is very small which is sufficient enough to perturb the whole surface into fragments. This is supported by the enlarged width and reduced intensity of the (400) peak (Fig. 1b). At 10 mA/cm^2 , pore formation starts and the entire surface shows sponge like structure. This is evident from the broad peak at 69.8° revealing an amorphous like nature but at the same location, where the single crystalline peak is also observed. The broad peak is shifted to lower 2θ value. This characteristic confirms the nanocrystalline silicon particles formation inside the pores after effecting some dissolution at the surface. When the current density is increased to 45 mA/cm^2 , the top portion of PSi structure is dissolved and the bottom surface near to the silicon substrate is exposed. Here, the particles will be slightly larger in size. This is explicit from the increased intensity and reduced width (FWHM) of the (400) peak. At very high current densities (60 mA/cm^2), dissolution of the top porous surface takes place and the inner silicon surface with large number of pits and larger silicon grains is exposed. This is confirmed by the appearance of the broad feature at the (400) plane along with a small peak.

The presence of peak with the (400) plane and the recorded shift to lower angles, as can be easily observed from Fig. 1, confirm that the cubic structure of the starting single crystal silicon is retained even in all porous structures [9]. This observed shift is in accordance with the results of XRD rocking curves obtained by Buttard et al. [10] in which two sharp peaks pertaining to Si substrate and PSi layer are present. In

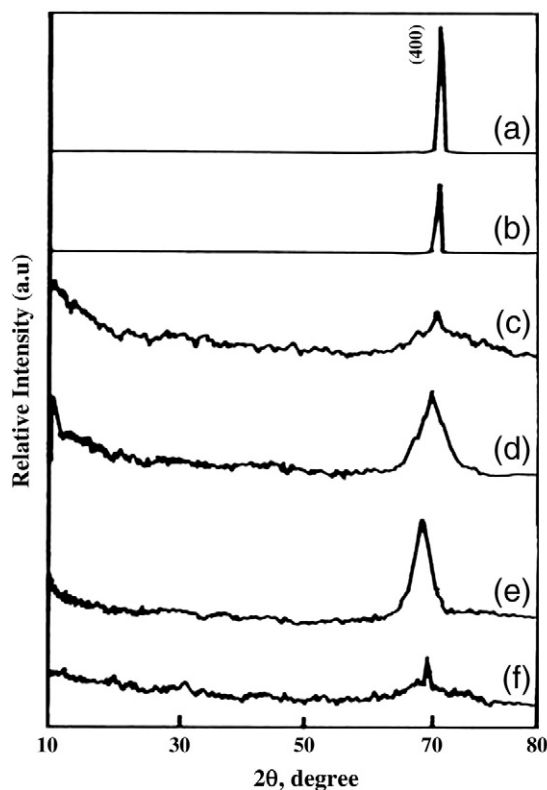


Fig. 1. XRD pattern of (a) single crystal silicon and PSi structures formed at (b) 5 (c) 10 (d) 30 (e) 45 and (f) 60 mA/cm^2 .

the case of the SnO_2 coated PSi, it is expected that a very thin layer of SnO_2 is formed over the PSi structure after filling the pores as well. To ascertain the incorporation of SnO_2 into the pores, XRD studies are conducted and shown in Fig. 2. The peaks pertaining to PSi are seen at 69.9° (400) along with the SnO_2 peaks at 26.8° (110) and 57.5° (002). These observations are in good agreement with the results observed for nanocrystalline SnO_2 powder [11] and pulse laser deposited (PLD) SnO_2 films on Si (100) substrates [12].

The nanocrystallite size in PSi layers and its distribution depend on the etching current density. The surface morphology observed by AFM for these PSi structures formed at current densities of 5, 10, 30, 45 and 60 mA/cm^2 is shown in Fig. 3a, b, c, d and e respectively.

The silicon nanorods are vertically aligned and evenly distributed over the entire surface as seen in Fig. 3c and d. The average diameter of these nanorods is about 30 nm. Both three dimensional and two dimensional (inset) morphologies are presented in Fig. 3c and d.

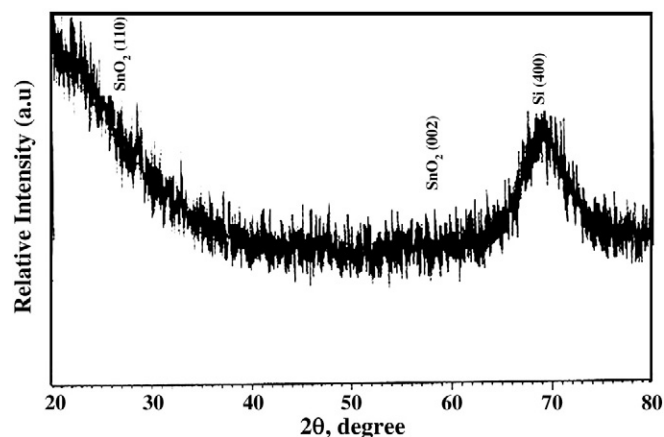


Fig. 2. XRD pattern of SnO_2 /PSi structure.

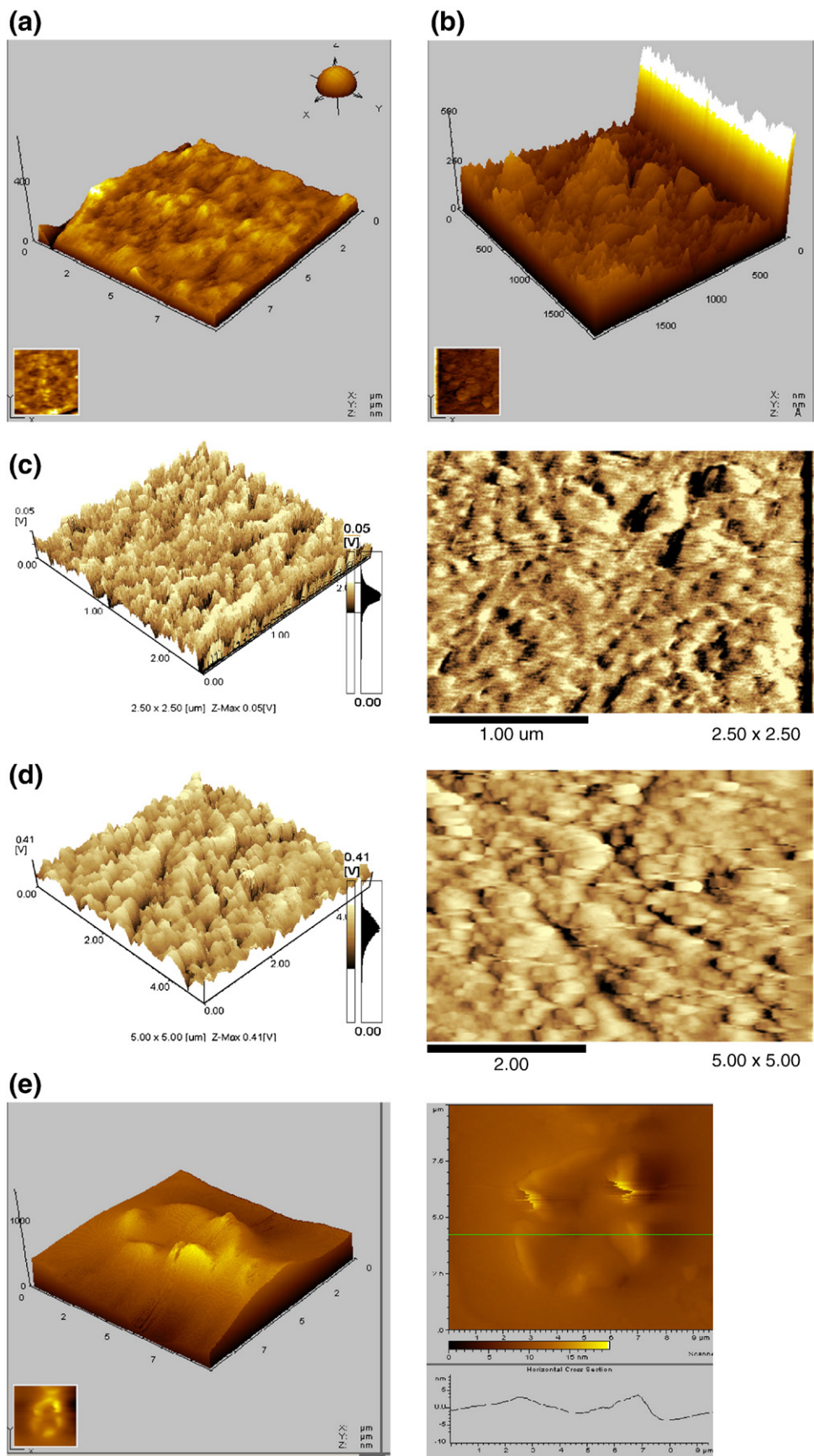


Fig. 3. AFM pictures of PSi structures formed with current densities of (a) 5 (b) 10 (c) 30 (d) 45 and (e) 60 mA/cm².

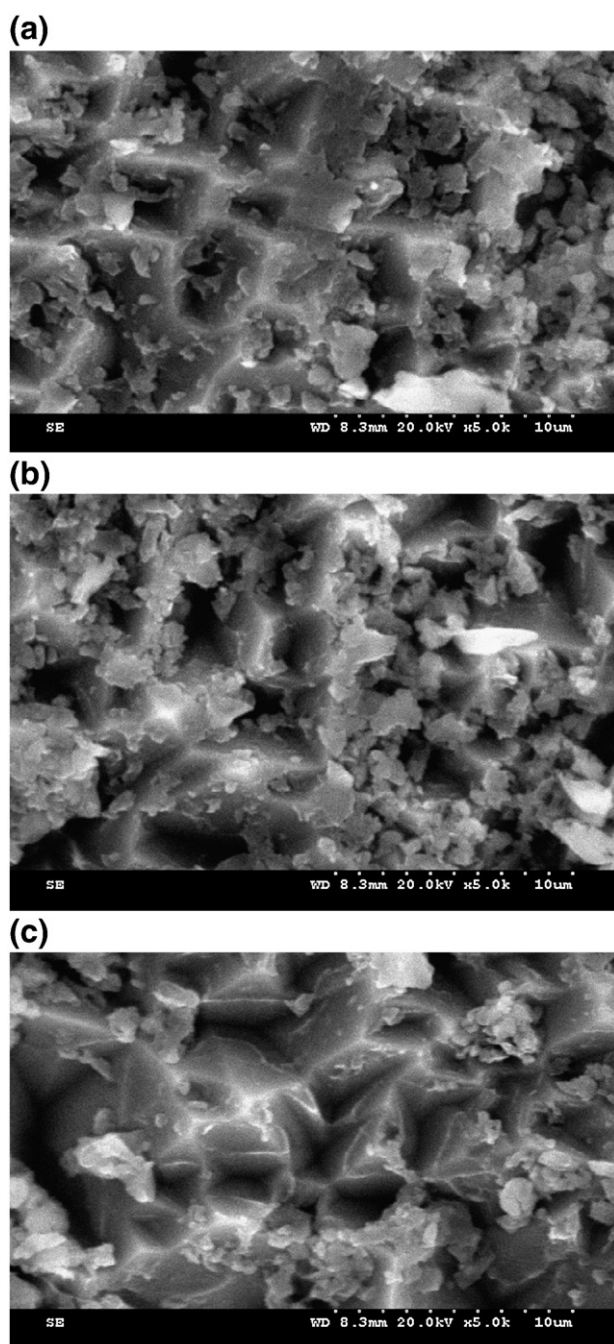


Fig. 4. SEM images of uncoated PSI structures formed at different current densities of (a) 30, (b) 45 and (c) 60 mA/cm².

Fig. 3a shows the initiation of silicon etching at 5 mA/cm² with larger grains. In Fig. 3b, the etching process at 10 mA/cm² has produced surface hillocks, possibly generated from the removal of silicon leaving this non-uniform nanostructures. In Fig. 3c, uniform and very fine needle like silicon (nanorods) nanostructures are observed which is the result of the best PSI structure formed at 30 mA/cm². The surface topography is the top portion of the first etched silicon surface which shows a mixed feature with less asperities and incipient porous structure. Fig. 3d shows thicker silicon pillars which are observed after the dissolution of the top fine porous layer at higher current densities beyond 30 mA/cm² [13,14]. This shows that the average pore depth increases with current density as explained by Chang and Chen [15]. These observations confirm the formation of nano-crystalline silicon particles inside the pores and all over the etched layers. It gives rise to photoluminescence at room

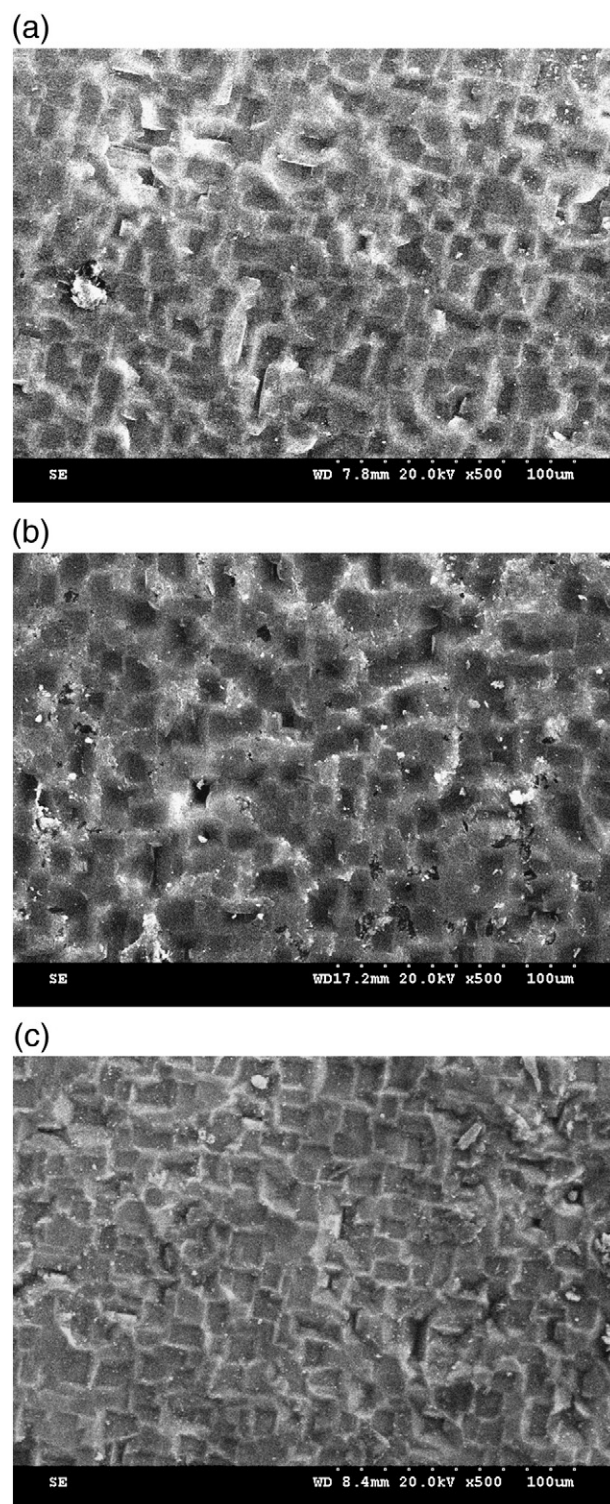


Fig. 5. SEM images of heat treated SnO₂/PSi heterojunctions deposited on PSI formed at different current densities of (a) 30, (b) 45 and (c) 60 mA/cm².

temperature which can be attributed to the quantum confinement effects (QCEs) owing to the presence of silicon nanocrystals in the etched layers [16]. Fig. 3e shows a single pit morphology with its thick silicon network. The horizontal cross section shows a pore diameter of about 4.5 µm formed at a high current density of 60 mA/cm².

Fig. 4a, b and c shows the SEM surface morphology of uncoated PSI formed at different current densities of 30, 45 and 60 mA/cm². It reveals increasing pore size with etching current density. These SEM results confirm the AFM observations, presented earlier.

Sol-gel precursors for SnO₂ formation were filled on PSi structure formed at 30, 45 and 60 mA/cm² and then heated at 400 °C for 15 min to form the SnO₂/PSi heterojunction. Fig. 5a, b and c shows the SEM images of the heated SnO₂/PSi junctions. The morphology shows increased surface coverage of the silicon pillars and edges of the pores.

Visual observation of the PSi showed golden brownish areas for various current densities. The observed PL spectra at room temperature for all the current densities confirm the formation of PSi structures with nanocrystalline features. PL spectra were recorded using a 365 nm excitation spectrum corresponding to an energy of 2.7 eV. The PL spectra are observed at higher wavelengths greater than 425 nm.

Fig. 6 shows the PL spectra of PSi structures formed at 5, 10, 30, 45, 60 mA/cm² for 10 min. The corresponding peaks are observed at 697, 654, 628, 649 and 643 nm respectively. It shows a bandgap turning with etching current (1.78 to 1.93 eV). The intensity increases up to 30 mA/cm² and then decreases. The PL spectra of PSi structures formed at 30 mA/cm² and etched for different durations were measured. The PL spectra exhibited maximum intensity for 10 min etching at different current densities.

At 30 mA/cm², a single-peak profile (Fig. 6c) shows the formation of silicon nanocrystallites uniformly distributed over the entire surface. The PSi samples prepared at current densities above and below 30 mA/cm² exhibit PL spectra with asymmetric and overlapped peaks. It means that, in these cases the PSi surface profile consists of a set of semi-isolated silicon nanocrystallites with different dimensions or shapes [17].

The PL spectra of the as prepared and heat treated SnO₂/PSi heterojunctions along with those of SnO₂ powder and uncoated PSi are shown in Fig. 7. The PL emission spectrum of the SnO₂ powder is shown in Fig. 7a. Two peaks are observed at 425 nm and 450 nm. These may be assigned to native defects such as oxygen vacancies or tin interstitials [18]. The PL spectra of bare PSi exhibited a single peak at 628 nm (Fig. 7b). The as prepared SnO₂/PSi junction shows a broad peak at 710 nm (Fig. 7c). After heat treatment at 400 °C for 15 min, the PL spectra shift to the blue region with a peak at 633 nm and a small hump

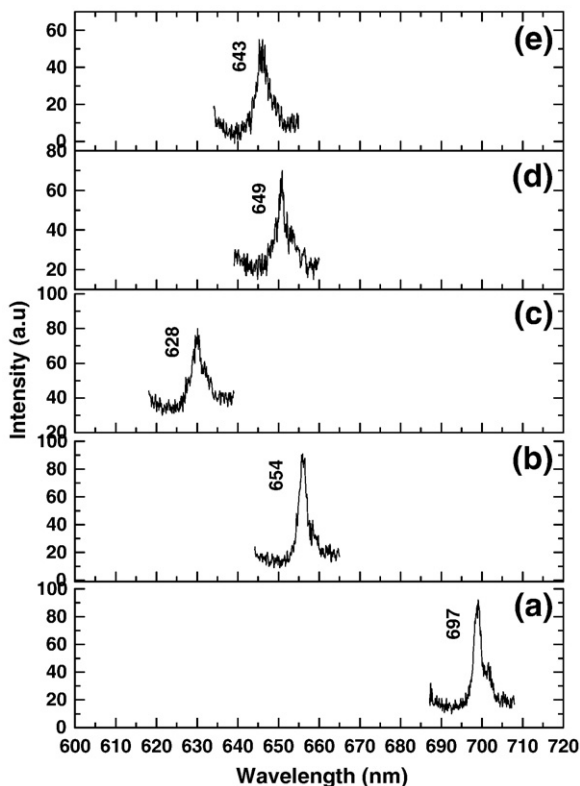


Fig. 6. Photoluminescence spectra of PSi structures formed at (a) 5, (b) 10, (c) 30, (d) 45 and (e) 60 mA/cm².

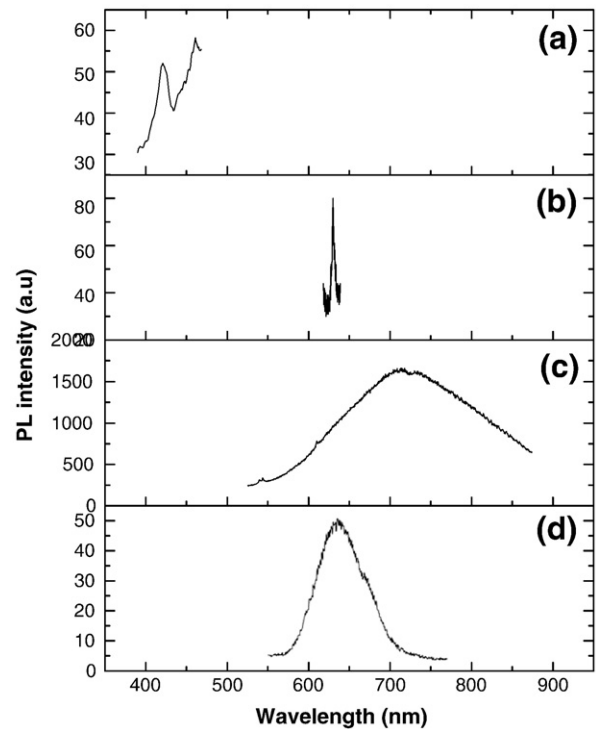


Fig. 7. Photoluminescence spectra of (a) SnO₂ powder (b) uncoated PSi (c) SnO₂/PSi heterojunction and (d) SnO₂/PSi heterojunction after heat treatment at 400 °C.

at about 660 nm. This may be due to the incorporation of SnO₂ into the pores and the blue shift may be due to the slightly enlarged shape and size of PSi coated with SnO₂ over the silicon pillars. This is also confirmed by the XRD and SEM results (Fig. 4). In the XRD pattern, peaks pertaining to SnO₂ and PSi are observed showing the formation of well adherent SnO₂ film on the silicon pillars and pore walls.

4. Conclusions

Steps to produce PSi layer with desired properties are optimized. PSi formed at 30 mA/cm² shows that it can be used effectively in the development of solar cells. The XRD, AFM and PL studies confirm the presence of silicon nanocrystallites and networks in the PSi structure.

References

- [1] R.L. Smith, S.D. Collins, *J. Appl. Phys.* 71 (1992) R1.
- [2] A. Halimaoui, in: J.C. Vial, J. Derrien (Eds.), *Porous Silicon Science and Technology* Les Editions de Physiques, Les Ullis, 1994, p. 33, and references therein.
- [3] L.T. Canham, *Appl. Phys. Lett.* 57 (1990) 1046.
- [4] C. Pickering, M.I.J. Beale, D.J. Robbins, *Thin Solid Film* 125 (1985) 157.
- [5] S. Bastide, M. Cuniot, P. Williams, Q.N. Le, D. Sarti, C. Levy-Clement, Proc. 12th EPSEC, H.S. Stephens and Associates, Amsterdam, 1994, p. 780, 1.
- [6] S. Strehlke, D. Sarti, A. Kroktus, K. Grigoros, C. Levy-Clement, *Thin Solid Films* 297 (1997) 291.
- [7] K. Luongo, A. Sine, S. Bhansali, *Sens. Actuators B* 111 (112) (2005) 125.
- [8] F. Rahimi, A. Irajizad, *Sens. Actuators B* 115 (2006) 164.
- [9] D. Bellet, G. Dolino, *Thin Solid Films* 276 (1996) 1.
- [10] D. Buttard, D. Bellet, G. Dolino, T. Baumbach, *J. Appl. Phys.* 83 (1998) 5814.
- [11] L. Abello, B. Bochu, A. Gaskov, S. Koudryatseva, G. Lucazeau, M. Roumyantseva, *J. Solid State Chem.* 135 (1998) 78.
- [12] Z.W. Chen, J.K.I. Lai, C.H. Shek, H.D. Chen, *Appl. Phys. A* 81 (2005) 1073.
- [13] U. Gosele, V. Lehmann, in: Z.C. Feng, R. Tsu (Eds.), *Porous Silicon*, World Scientific, Singapore, 1994, p. 17.
- [14] S.D. Campbell, L.A. Jones, E. Nakamichi, F.-X. Wei, L.D. Zajchowski, D.F. Thomas, *J. Vac. Sci. Technol. B* 15 (1995) 1184.
- [15] M. Chang, Y.F. Chen, *J. Appl. Phys.* 82 (1997) 3514.
- [16] D.A. Kim, S.I. Im, C.M. Whang, W.S. Cho, Y.C. Yoo, N.H. Cho, J.G. Kim, Y.J. Kwon, *Appl. Surf. Sci.* 230 (2004) 125.
- [17] H.S. Mavi, B.G. Rasheed, R.K. Soni, S.C. Abbi, K.P. Jain, *Thin Solid Films* 397 (2001) 125.
- [18] T.W. Kim, D.U. Lee, Y.S. Yoon, *J. Appl. Phys.* 88 (2000) 3759.